Single cell patterning for high throughput toxicity assay

Description of Technology

A panel of in vitro toxicity assays has been developed to assess the effects of chemicals and external stimuli on cultured mammalian cells for drug screening and hazard identification. [1-4] The toxicity assays depend on cell functions such as enzyme activity, membrane permeability, adherence, adenosine triphosphate (ATP) and co-enzyme productions, and nucleotide uptake activity. [5-7] The assays can provide averaged signals from a large population of cells. However, due to cellular heterogeneity, the toxicity results derived from cell population can be irrelevant or misleading especially in the case of cancer which is known for high level of heterogeneity. [8-9] Cell population based toxicity assays cannot distinguish responses of single cells and sub-cellular organelles; while single cell assays are limited by low statistical power due to small number of cells examined. Moreover, single cell assay cannot provide long term tracking ability without live cell imaging system. This invention disclosure describes a new single cell array based toxicity assay, in which cell responses at population level, single cell level and sub-cellular level can be obtained simultaneously at high throughput, and individual cell can be tracked with array-embedded coordinate system (Figure 1). The single cell array with coordinate system was produced by microcontact printing and selected area cell attachment, and exposed to damaging X-ray radiation, which was followed by fluorescence imaging after staining. By physically attaching cells at the same height and ordered locations, the issues of cell overlapping and clustering associated with random distribution were solved completely, and there is no need for an user to change observation field to find cells that can provide useful information. Image processing software written in MATLAB were used to determine the DNA content and production of reactive oxygen species (ROS). The results showed significant differences in responses at single cell level in a large population of cells upon exposure to radiation. By uniquely providing population-based assay with sub-cellular spatial resolution and single cell sensitivity, this method has the potential to significantly impact the toxicity field.

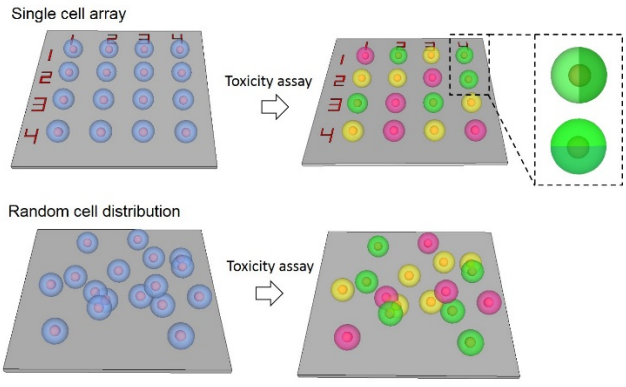

Figure 1. Single cell patterning for high throughput toxicity assay

Novel and Unusual Features

- Low-cost cell tracking in toxicity assay
- Compatible with Cartesian, polar, cylindrical and spherical coordinate systems

- Automated cell array image processing
- Toxicity information at sub-cellular, single cell and population levels

Advantages and Improvements over existing methods, devices, or materials

- Relocate the same cell after drug treatment in toxicity assay
- Real time cell tracking without live cell imaging system or other labelling techniques
- Simultaneous acquisition of toxicity information at sub-cellular, single cell and population levels

Commercial Applications

- Single cell genomic analysis
- Single cell proteomic analysis
- Single cell PCR

Technical Description

1. Materials and methods

Poly(allylamine hydrochloride) (PAH) with molecular weight of 120,000-200,000 was from Alfa Aesar. Poly(sodium 4-styrene sulfonate) (PSS) with molecular weight of 70,000, fluorescein isothiocyanate isomer I (FITC), Hydroxy(polyethyleneoxy) propyl triethoxysilane (PEG-silane) (8-12 ethylene oxide, 50% in ethanol) was from Gelest. Polydimethylsiloxane (PDMS Sylgard 184) was from Dow Corning. Hoechst 33342, and Carboxy-H2DCFDA were from ThermoFisher. Polyelectrolyte stock solutions were 1 wt% PAH at pH 10, 1 wt% PSS at pH 5.8, and 1% PAH at pH 5.8, all contain 150 mM NaCl.

A mixture of PDMS prepolymer and curing agent (10:1 weight ratio) was poured onto a master prepared by photolithography. After being kept at 37 °C for 24 h, the solidified PDMS slab was peeled off and cut into square stamps that have vertical micro-pillars with a diameter of 10 μm, a height of 5 μm, and a center-to-center distance of 30 μm in the hexagonal lattice. A glass slide was treated with high level oxygen plasma for 3 min, and soaked in PEG-silane solution (5% in ethanol) for overnight, and rinsed with water and dried with an air stream.

Single cell array is formed as follows. A PDMS stamp with micropillars was immersed in polyelectrolyte solution for 15 min and rinsed with water to form multilayers. After drying in air, the stamp was exposed to vapor from a water bath, and immediately brought into contact with a PEG-coated slide for 20 min to allow water between stamp and slide to evaporate, which is followed by peeling off the stamp to complete the pattern transfer. To enclose cell suspension onto the patterned substrate, a PDMS slab with a 5 mm diameter hole was placed on the pattern to form a chamber, into which 200 μL cell suspension in culture medium was added. The cells in chamber was incubated at 37 °C and 5% CO2 for 1 h, followed by removing PDMS slab and washing the slide with phosphate buffer saline (PBS) to remove unbound cells.

HeLa cells were cultured in DMEM medium supplemented with 10% fetal bovine serum (FBS), 100 units/mL of penicillin at 37 °C and 5% CO2. For DNA damage assay, arrayed cells were stained by Hoechst 33342 at final concentration of 10 μM for 10 min, and irradiated with X-ray at 20 GY. For ROS detection, carboxy-H2DCFDA was added to arrayed cells at final concentration of 20 μM. After incubation for 30 min and washed with PBS, cells were irradiated with X-ray at 20 GY dosage.

2. Results and discussion

PAH is positively charged at neutral pH and can be adhesive to cells since many types of mammalian cells are negatively charged due to existence of sialic acid on their surfaces. [10] PEG-coated surface is well known for its anti-fouling property and can prevent adhesion of cells. [11] Figure 2A shows a 5×5 array of multilayers composed of PAH/PSS/PAH-FITC printed on a PEG-coated glass slide. Each region is uniquely labelled and consists of 30×30 10 μm sized microdots. Figure 2B shows array of HeLa cells. The size of each micropatch is 10 μm, and the center-to-center distance is 30 μm, thus each patch can capture one cell without bridging two adjacent patches.

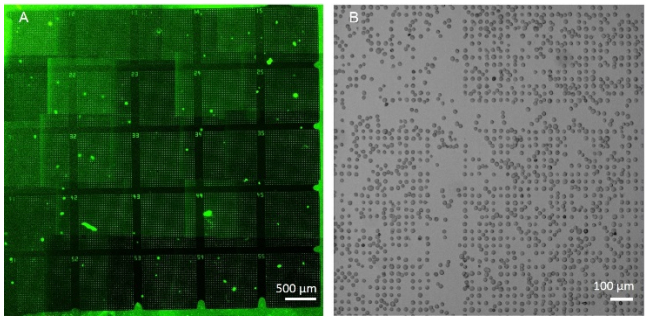

Figure 2. Array of PAH/PSS/PAH-FITC on PEG (A). Single cell array of HeLa cell (B).

Arrayed HeLa cells were exposed to ionizing X-ray radiation from a generator operated at 115 kV and 5 mA. The impacts of radiation on genomic integrity and reactive oxygen species (ROS) production were quantitatively analyzed. Figure 3A and 3B shows Hoechst staining of DNAs in arrayed cells before and after radiation at the same location. Figure 3C is the micropattern with coordinates for locating cells. The fluorescence intensity is lower after radiation because of double strand break and low binding capacity of Hoechst to single-stranded DNA. [12] A major advantage of single cell array is that it allows for image-based analysis of a large population of cells by software. MATLAB was used to quantify fluorescence intensity of individual cell. Figure 3D shows fluorescence intensity before and after radiation of each individual cell. Figure 3E shows histogram of change in fluorescence intensity of arrayed cells.

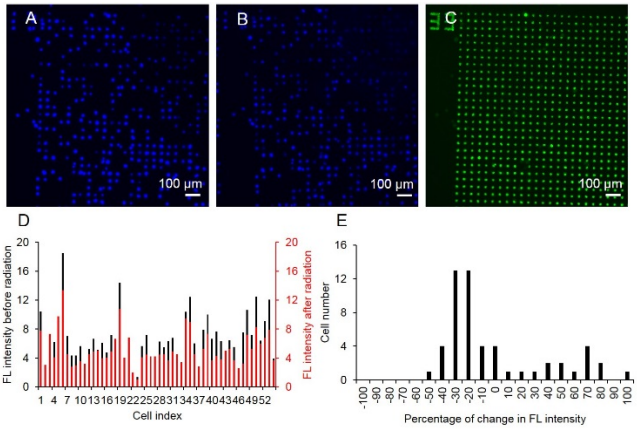

Figure 3. Nuclei staining of arrayed HeLa cell before (A) and after (B) X-ray radiation (dosage: 20 GY) and corresponding cell coordinate (C). Fluorescence intensity of nuclei of arrayed cell before and after radiation (D). Histogram of percentage of change in fluorescence intensity (E). Negative value means decrease and positive value means increase.

Radiation induced oxidative stress can also damage cells and cellular organelles, therefore can be assessed on a single cell array. Figure 4A and 4B shows ROS detection before and after radiation. The fluorescence intensity becomes higher after radiation due to production of ROS. Figure 4D shows plot of fluorescence intensity before and after radiation of each individual cell. Figure 3E shows histogram of change in fluorescence intensity of arrayed cells.

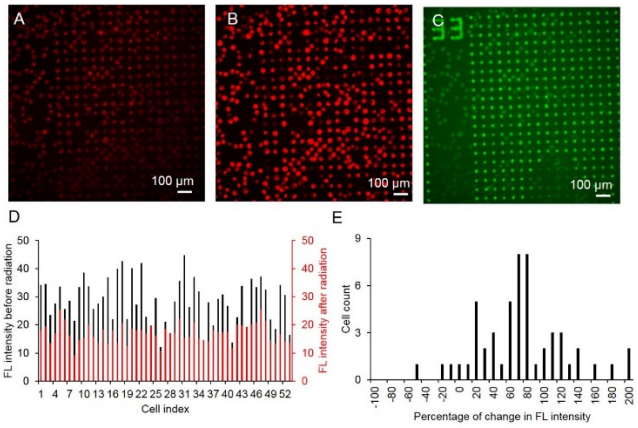

Figure 4. ROS staining of arrayed HeLa cell before (A) and after (B) X-ray radiation (dosage: 20 GY). Fluorescence intensity of arrayed cell before and after radiation (E). Histogram of percentage of change in fluorescence intensity (F). Negative value means decrease and positive value means increase.

References

[1] R.H. Shoemaker, The NCI60 human tumour cell line anticancer drug screen, Nat. Rev. Cancer, 6 (2006) 813-823.

[2] C. Lam, J.T. James, R. McCluskey, S. Arepalli, R.L. Hunter, A review of carbon nanotube toxicity and assessment of potential occupational and environmental health risks, Crit. Rev. Toxicol., 36 (2008) 189-217.

[3] C.F. Jones, D.W. Grainger, In vitro assessments of nanomaterial toxicity, Adv. Drug Deliv. Rev., 61 (2009) 438-456.

[4] Q. Wang, Y. Bao, X. Zhang, P.R. Coxon, U.A. Jayasooriya, Y. Chao, Uptake and toxicity studies of poly-acrylic acid functionalized silicon nanoparticles in cultured mammalian cells, Advanced healthcare materials, 1 (2012) 189-198.

[5] J. Sikkema, J.A.M. Bont, B. Poolman, Mechanisms of membrane toxicity of hydrocarbons, Microbiol. Rev., 59 (1995) 201-222.

[6] P.V. AshaRani, G.L.K. Mun, M.P. Hande, S. Valiyaveettil, Cytotoxicity and genotoxicity of silver nanoparticles in human cells, ACS Nano, 3 (2009) 279-290.

[7] D. Fischera, Y. Li, B. Ahlemeyerc, J. Krieglsteinc, T. Kissel, In vitro cytotoxicity testing of polycations: influence of polymer structure on cell viability andhemolysis, Biomaterials, 24 (2003) 1121-1131.

[8] M.S. Lawrence, P. Stojanov, P. Polak, G.V. Kryukov, K. Cibulskis, A. Sivachenko, S.L. Carter, C. Stewart, C.H. Mermel, S.A. Roberts, A. Kiezun, P.S. Hammerman, A. McKenna, Y. Drier, L. Zou, A.H. Ramos, T.J. Pugh, N. Stransky, E. Helman, J. Kim, C. Sougnez, L. Ambrogio, E. Nickerson, E. Shefler, M.L. Cortes, D. Auclair, G. Saksena, D. Voet, M. Noble, D. DiCara, P. Lin, L. Lichtenstein, D.I. Heiman, T. Fennell, M. Imielinski, B. Hernandez, E. Hodis, S. Baca, A.M. Dulak, J. Lohr, D.A. Landau, C.J. Wu, J. Melendez-Zajgla, A. Hidalgo-Miranda, A. Koren, S.A. McCarroll, J. Mora, R.S. Lee, B. Crompton, R. Onofrio, M. Parkin, W. Winckler, K. Ardlie, S.B. Gabriel, C.W. Roberts, J.A. Biegel, K. Stegmaier, A.J. Bass, L.A. Garraway, M. Meyerson, T.R.

Golub, D.A. Gordenin, S. Sunyaev, E.S. Lander, G. Getz, Mutational heterogeneity in cancer and the search for new cancer-associated genes, Nature, 499 (2013) 214-218.

[9] J.M. Raser, E.K. O'Shea, Noise in gene expression: origins, consequences, and control, Science, 309 (2005) 2010-2013.

[10] E.I. Finkelstein, P.H. Chao, C.T. Hung, J.C. Bulinski, Electric field-induced polarization of charged cell surface proteins does not determine the direction of galvanotaxis, Cell Motil. Cytoskel., 64 (2007) 833-846.

[11] Z. Wang, P. Zhang, B. Kirkland, Y. Liu, J. Guan, Microcontact printing of polyelectrolytes on PEG using an unmodified PDMS stamp for micropatterning nanoparticles, DNA, proteins and cells, Soft Matter, 8 (2012) 7630-7637.

[12] C. B. Khan, U. Hentschel, Y. Nikandrova, J. Krug, G. Horneck, Fluorometric analysis of DNA unwinding (FADU) as a method for detecting repair-induced DNA strand breaks in UV-irradiated mammalian cells. Photochem. Photobiol. 72 (2000) 477-484.